Chinese Chemical Letters 32 (2021) 2359–2368

Contents lists available at ScienceDirect

Chinese Chemical Letters

journal homepage: www.elsevier.com/locate/cclet

Review

# Visible and near-infrared light activated azo dyes

Huijuan Chen[a,b], Weijie Chen[a,b], Yan Lin[d], Yuan Xie[c], Sheng Hua Liu[a,b], Jun Yin[a,b,c,*]

[a] Key Laboratory of Pesticide and Chemical Biology, Ministry of Education, Hubei International Scientific and Technological Cooperation Base of Pesticide and Green Synthesis, International Joint Research Center for Intelligent Biosensing Technology and Health, College of Chemistry, Central China Normal University, Wuhan 430079, China
[b] Ministry of Education Key Laboratory for the Synthesis and Application of Organic Functional Molecules, Hubei University, Wuhan 430062, China
[c] Guangdong Provincial Key Laboratory of Radioactive and Rare Resource Utilization, Shaoguan 512026, China
[d] Department of Pharmacy, Jiangxi University of Traditional Chinese Medicine, Nanchang 330013, China

ARTICLE INFO

*Article history:*
Received 9 January 2021
Received in revised form 4 March 2021
Accepted 5 March 2021
Available online 9 March 2021

*Keywords:*
Photochromism
Azo dyes
Visible light activation
Near-infrared light activation

ABSTRACT

The photoisomerization properties of azo derivatives have been widely used in the fields of materials and biology. One serious restriction to the development of functional azo-based materials is the necessity to trigger switching by UV light, which damage the corresponding surfaces and penetrate only partially through the matter. Therefore, developing the visible and near-infrared light activated azo switches can solve this problem. This review provides a summary of molecular design strategies for driving the isomerization of azo derivatives with visible light and near-infrared light: (1) smart design directly excited by visible light, (2) the addition of upconversion nanoparticles, (3) the employment of two-photon absorption, (4) indirect excitation in combination with metal sensitizer.


## 1. Introduction

Azo compounds are organic compounds that contain N=N double bonds. Azobenzene is the simplest aromatic azo compound and its synthesis can be traced back to 1834. However, it was only in 1937 that Hartley used UV light to irradiate azobenzene [1], and then the photoisomerization performance of azo compounds gradually gained importance.

With the development of azo compounds, some crucial parameters were used to assess their isomerization. The photoswitching performance is mainly characterized by the following four properties [2]: (i) Addressability. Including maximum absorption wavelength ($\lambda_{max}$), the gap between the maximum absorption wavelengths of *cis*- and *trans*-isomers ($\Delta\lambda$), and molar extinction coefficient ($\varepsilon$). (ii) Thermal stability. This can be expressed by the thermal half-life ($\tau_{1/2}$) of the unstable isomer under certain conditions. Based on to the magnitude of $\tau_{1/2}$, photoswitches can be divided into T-type ($\tau_{1/2}$ ranging from milliseconds to seconds) and P-type (no or very slow thermal isomerization). (iii) Efficiency. This property is characterized by the number of the photons used for isomerization ($\varphi$) and the degree of conversion in the photostationary state (PSS). (iv) Reliability. This measures how often a photoswitch can isomerize without significant degradation under adverse side reaction conditions.

The above-described properties of azo compounds can be effectively modified by changing the substituents to obtain compounds that are suitable for applications in different fields. For example, materials for optical data storage require high thermal stability [3]. For application in real-time information transmission, push-pull azobenzenes that display fast thermal conversion from *cis*-isomer to *trans*-isomer are often used, in order to avoid the second light stimulation of the sample [4], while a combination of bridged azobenzenes and pharmaceuticals is favored in photopharmacology [5].

To date, azo compounds have been widely investigated in materials science [6] and biology [7,8]. Although azo compounds have shown excellent switchable performance, most azo compounds still need to be activated by UV light. Unfortunately, the UV light necessary to activate azo switches occupies only a small portion of the UV–vis absorption spectra, and short-wavelength UV light also has display high scattering and weak penetrability [9,10]. In addition, high-energy UV light can cause great damage to the surface of the substance [11,12]. Therefore, the construction of azo compounds for which photoisomerization occurs in the visible and near-infrared regions is an important research direction. To date, four approaches have been mainly used to obtain azo compounds activated by visible and near-infrared light: (1)

* Corresponding author at: Key Laboratory of Pesticide and Chemical Biology, Ministry of Education, Hubei International Scientific and Technological Cooperation Base of Pesticide and Green Synthesis, International Joint Research Center for Intelligent Biosensing Technology and Health, College of Chemistry, Central China Normal University, Wuhan 430079, China.
*E-mail address:* yinj@mail.ccnu.edu.cn (J. Yin).

https://doi.org/10.1016/j.cclet.2021.03.020
1001-8417/

modification of azo compounds to enable their direct excitation by visible and near-infrared light, (2) the addition of upconversion nanoparticles, (3) the employment of two-photon absorption, (4) indirect excitation in combination with metal sensitizer. In this review, we summarize the recent progress in the development of visible and near-infrared activated azo compounds using these approaches.

## 2. Direct visible light excitation

Based on the excitation characteristics of the n→$\pi^*$ and $\pi$→$\pi^*$ transitions, azo compounds can be roughly divided into three categories of azobenzenes, aminoazobenzenes, and pseudostilbenes (Fig. 1) [13,14].

For aminoazobenzenes, their $\pi$→$\pi^*$ transition redshifts and overlaps with the absorption due to the n→$\pi^*$ transition, and the difference in the molar extinction coefficient between the two bands is small. The energies of the $\pi$→$\pi^*$ and n→$\pi^*$ transitions in pseudostilbenes are similar and both transition occur in the visible-light region. The energy of the $\pi$→$\pi^*$ transition can be adjusted to become even be lower than that of the n→$\pi^*$ transition by either raising the n→$\pi^*$ energy (protonated azobenzenes, $BF_2$ azobenzenes) or by lowering the $\pi$→$\pi^*$ energy (push-pull azobenzenes). For the latter two types of azo compounds, the $\pi$→$\pi^*$ and n→$\pi^*$ bands tend to overlap, and thermal isomerization is fast. It is often difficult to selectively irradiate one isomer and achieve a highly enriched PSS.

The $\pi$→$\pi^*$ band of *trans*-azobenzene without any substituents is located in the UV region ($\lambda_{max}$ = ~320 nm, $\varepsilon$ = ~22,000 L $mol^{-1}$ $cm^{-1}$), and its n→$\pi^*$ band is found in the visible region ($\lambda_{max}$ = ~450 nm, $\varepsilon$ = ~400 L $mol^{-1}$ $cm^{-1}$). Compared to *trans*-azobenzene, the $\pi$→$\pi^*$ transitions of *cis*-azobenzene ($\lambda_{max}$ = ~270 nm, $\varepsilon$ = ~5000 L $mol^{-1}$ $cm^{-1}$) are weaker, and n→$\pi^*$ transitions ($\lambda_{max}$ = ~450 nm, $\varepsilon$ = ~1500 L $mol^{-1}$ $cm^{-1}$) are stronger [13]. The difference between the $\pi$→$\pi^*$ bands of the *cis*- and *trans*-isomers is greater than that between their n→$\pi^*$ bands. Therefore, UV light is used instead of visible light to achieve *trans*-to-*cis* photoswitching. Reverse (*cis*-to-*trans*) photoswitching can be accomplished with blue light or by thermal relaxation. The photophysical properties of the molecules involved in the photoswitching are shown in Figs. 2 and 3.

### 2.1. o-Haloazobenzenes

In 2012, Hecht *et al*. found that azobenzene **1** containing four electron-withdrawing fluorine atoms on *ortho* positions of azo unit could reduce the n-orbital energy of *cis*-isomer, leading to the blue-shift of n→$\pi^*$ in *cis*-**1**. In acetonitrile, the maximum absorption of **1** was found at 458 nm while that of the *cis*-**1** isomer was found at 414 nm. The separation of n→$\pi^*$ transition is 42 nm, so green light (> 450 nm) and blue light (410 nm) could be used to drive the *trans*-to-*cis* and *cis*-to-*trans* photoisomerizations, respectively. Moreover, *cis*-**1** displayed a long thermal half-life that was as high as 700 days in DMSO [15]. Subsequently, Hecht *et al*. further explored the effect of *para*-substituents for the photoisomerization and investigate azobenzene **2** containing two electron-withdrawing groups (-COOEt) in the *para* positions with the electron-withdrawing groups cooperating with four fluorine atoms [16]. Compared to azobenzene **1**, the maximum absorption of *trans*-**2** redshifted to 469 nm, and the conversion rates ($PSS_{E→Z}$ = 90%, $PSS_{Z→E}$ = 97%) were greatly improved.

In addition to fluorine, other halogens (chlorine and bromine) also showed a strong effect on the photoisomerization of azo compounds such as *o*-chloroazobenzene (**3**) and *o*-bromoazobenzene (**4**) [17]. The flexible conformation of azobenzenes **3** and **4** led to the extension of their absorption bands to 600 nm. Therefore, **3** and **4** could be excited to carry out photoisomerization by red light in the 625−652 nm wavelength range. In 2019, Ochsenfeld *et al*. found that the absorption band of **5** extended to 650 nm and *trans*-to-*cis* isomerization was driven by red light at 660 nm when two chlorine atoms of **3** were replaced by fluorine atoms to form azobenzene **5** [18]. And Ochsenfeld *et al*. explained the effect of electrons and geometry on the photophysical properties of *o*-chloroazobenzenes by calculation. When the *ortho* position of the azo bond contains two or more chlorine atoms, due to steric hindrance, *o*-chloroazobenzenes are flexible and contain a variety of conformations. Red light is used to drive conformations at the end of the absorption spectrum. Because of the continuous conversion between conformations of *o*-chloroazobenzenes, coupled with the small spectral overlap of the *cis*- and *trans*-isomer at tail bands, long-term exposure to red light can gradually accumulate high *cis*-content PSS [18].

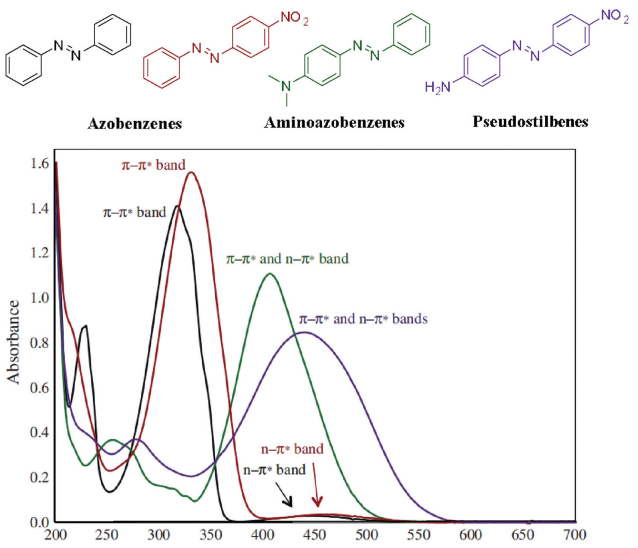


**Fig. 1.** The UV–vis absorption spectra of three types of azobenzenes. Copied with permission [14]. Copyright 2019, John Wiley and Sons.

Accordingly, *o*-haloazobenzenes are a typical class of azo compounds activated by visible light, facilitating their application in biological systems.

### 2.2. Bridged azobenzenes

In the previous century, it was reported that when weak electron-donating alkyl groups are introduced on the *ortho* positions of the azo unit, the formed azobenzenes can only undergo photoisomerization upon irradiation with UV light [19]. Bridged azobenzenes can be regarded as a special type of substituted azobenzenes with an alkyl at the *ortho* position of the azo unit [20]. When they were subjected to the changes in ring tension, the deformable macrocyclic azobenzenes exhibited unconventional characteristics such as visible light-driven photoisomerization, thermally stable *cis*-isomers, high quantum yield, and high photoconversion rate [21].

In 2009, Temps *et al*. first discussed the photoisomerization property of bridged azobenzenes. Compound **6** is the simplest bridged azobenzene and in *n*-hexane, the maximum absorption wavelength of its *trans*-isomer was found at 490 nm while the maximum absorption wavelength of *cis*-**6** was found at 404 nm. Irradiation at 385 nm leads to the conversion of more than 90% of *cis*-**6** to the *trans*-form, and *trans*-**6** can then be quantitatively converted to *cis*-isomer by irradiation with green light.

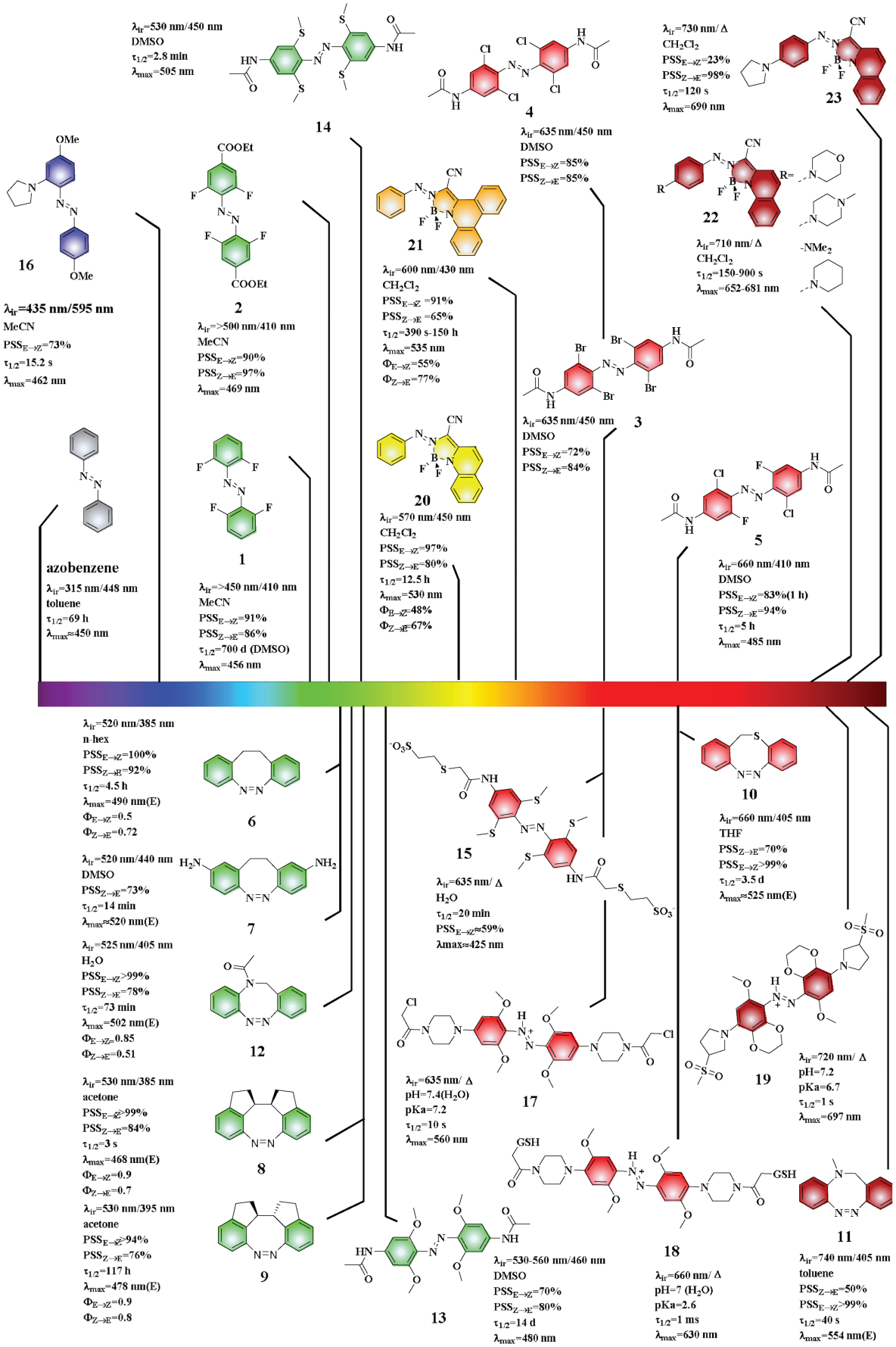


**Fig. 2.** Irradiation wavelength for isomerization of different types of azo compounds.

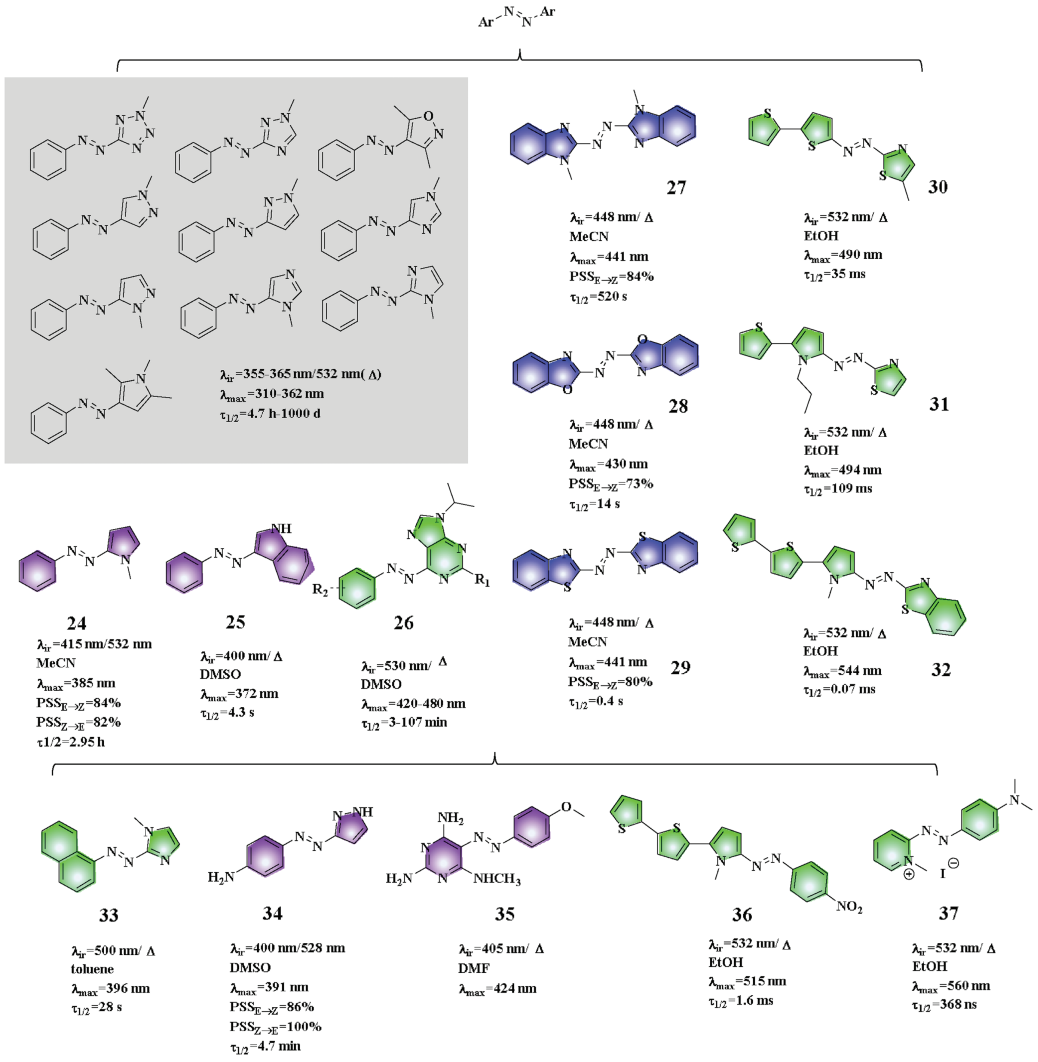


**Fig. 3.** Irradiation wavelength for isomerization of different types of heterocyclic azobenzenes.

The *cis*-isomers of most bridged azobenzene derivatives exhibit similar photophysical properties, and their maximum absorption wavelengths are generally located in the vicinity of 400 nm. The *cis*-to-*trans* isomerization of bridged azobenzenes is often excited by 385−440 nm light [22–24]. Based on the excellent performance of azobenzene **6**, some attempts mainly such as substitution on the benzene ring, and substitutions on the middle bridge ring have been carried out to extend the maximum absorption wavelengths of *trans*-isomers of bridged azobenzenes in recent years.

Trauner *et al.* [22] and Staubitz *et al.* [23] introduced different types of substituents on the benzene ring of the azobenzene unit that could induce the shift of the maximum absorption wavelengths of the *trans*-isomers to approximately 490 nm, enabling their excitation by green light. When a strong electron-donating group was introduced on the *para* position of the azo unit, the absorption bands of both the *cis*- and *trans*-isomers red-shifted. For example, two amino groups were simultaneously introduced on the *para* positions of the azo unit to form azobenzene **7** [22]. The maximum absorption of *trans*-**7** was observed at approximately 520 nm while that for *cis*-**7** in DMSO was observed at approximately 420 nm. Moreover, it was shown that illumination at 520 and 440 nm could drive the *trans*-to-*cis* and *cis*-to-*trans* isomerizations, respectively.

Starting with azobenzene **6**, in 2020 Herges *et al.* fused two five-membered rings with the ethylene bridge and two benzene rings to form meso molecule **8** and racemic molecule **9**, respectively [25]. In this case, each isomer had only one conformation. The maximum absorption wavelengths of *trans*-**8** and *trans*-**9** blue-shifted to 468 nm and 478 nm, respectively. Interestingly, both **8** and **9** achieved *trans*-to-*cis* isomerization under irradiation at 530 nm.

In consideration of the small red shifts obtained by the above method, Herges *et al.* subsequently used heteroatoms (*e.g.*, O, S, and N) to replace the carbon atom of the bridge ring. When an oxygen or sulfur atoms replaced a carbon of the bridge ring, the absorption of the *trans*-isomer showed a clear red-shift in comparison to **6** and both compounds had a maximum absorption wavelength of 525 nm. In particular, the *trans*-**10** absorption band extended to wavelengths higher than 700 nm and therefore, *trans*-to-*cis* isomerization could be achieved with 660 nm red light [21]. When one carbon atom on the bridge ring was substituted by a methylamino group, the absorption bands of *trans*-**11** extended to the wavelengths in the vicinity of 800 nm, enabling photoisomerization under near-infrared (740 nm) irradiation. In various aza-bridged azobenzenes, acetamidosubstituted bridged azobenzene (**12**) showed good water solubility, and its maximum absorption was observed at 502 nm in water, enabling

*cis*-to-*trans* isomerization by the irradiation of green light. Therefore, **12** was identified as a promising candidate for applications as a photoswitch in biochemistry and photopharmacology [26].

### 2.3. o-*Methoxyazobenzenes*

In 2011, Woolley *et al*. reported azobenzene **13** containing four electron-donating methoxyl groups on the *ortho* positions of the azo unit [27]. In DMSO, the maximum absorption of *trans*-**13** was found at 480 nm while the maximum absorption wavelength of *cis*-**13** was observed at 444 nm. Photochromism was driven by green light (530−560 nm) and light at 460 nm for the *trans*-to-*cis* and *cis*-to-*trans* isomerizations, respectively. However, azobenzene **13** was easily reduced by glutathione. Compared to **13**, the absorption of sulfur-containing azobenzene **14** red-shifted to wavelengths higher than 500 nm, and **14** showed good anti-reducing behavior in the presence of glutathione. Subsequently, the *para*-substituent of **14** was modified to afford azobenzene **15** for which the absorption band extended to 600 nm, allowing photoisomerization triggered by red light (635 nm) [28].

### 2.4. Aminoazobenzenes

Azobenzenes with one or more amino or hydroxyl substituents at the *para*- or *ortho*-positions of the azo unit are called aminoazobenzenes. The number of substituents, degree of amino alkylation, and polarity of solvents can affect their absorption. Generally, *para*- and *ortho*-substitution were found to have stronger influence than *meta*-substitution. When the amino or hydroxy substituents were not completely alkylated, they easily formed intramolecular hydrogen bonds with the azo group, causing the loss of photochromic activity [13].

Woolley [29] and Priimagi [30] introduced a series of amine groups on the *ortho* position of the azo unit. The maximum absorption wavelength of pyrrole substituted azobenzene **16** was 462 nm. It was found that as the number of electron-donating groups increases, the absorption shifts to the green region.

### 2.5. Push-pull azobenzenes

By introducing an electron-withdrawing group on one benzene ring and an electron-donating group on the other benzene ring, a push-pull azobenzene can be formed, redshifting the maximum absorption wavelength to the visible light region [31]. However, in many cases, the thermal stability of metastable isomers drops sharply and PSS of push-pull azobenzenes has low contents for each isomer ($PSS_{E\rightarrow Z} \leq 82\%$, $PSS_{Z\rightarrow E} \leq 95\%$) [32]. Therefore, without a specialized laser flash photolysis apparatus, it may be difficult to observe photoisomerization of some push-pull azobenzenes. In addition, due to their good nonlinear optical properties, push-pull azobenzenes can be used with near-infrared two-photon absorption, and thus can be used in practical applications with deeper penetrating near-infrared light [33].

### 2.6. Protonated azobenzenes

Protonation can further redshift the absorption of azo derivatives. Generally, the p*K*a value of azo ions is between 1.5 and 3.5 [34], but the p*K*a values of heterocyclic azobenzenes may be slightly higher (azoimidazole: p*K*a = 4.7 [35]). In a near neutral biological environment, azo ions are often absent or their content is low. In this case, protonated *o*-methoxy azo compounds achieve *cis*-*trans* isomerism in near neutral environments.

Woolley *et al*. conducted a preliminary examination of the apparent p*K*a value of **13**. It was found that due to the intramolecular hydrogen bond between *o*-methoxy and the nitrogen atom on the azo bond, and the resonance stabilization of azo ions, the apparent p*K*a value increased compared to other types of azo compounds, and protonation occurred at pH 3 [27]. The realization of protonation under physiological conditions lays the foundation for the use of azo derivatives in cells and even living bodies. Following this principle, the four methoxy groups in the *ortho* position were retained, and a strong electron-donating group was introduced at the *para* position to form azobenzene **17** with a further increased alkalinity and the apparent p*K*a of 7.2 [34]. The maximum absorption wavelength of **17** was 560 nm, and **17** was sensitive to red light under physiological conditions. Then, through the introduction of the second auxiliary chromophore on the *meta* position, the absorption could be further red-shifted [36]. In the structure of **18** ($\lambda_{max}$ = 630 nm), the two *ortho* methoxy groups were moved to the *meta* position. However, the presence of the *meta* substituent forced the *para*-piperazine to rotate, and the removal of the *o*-methoxy group reduced the azo ion resonance stability, so that the ability of the *para* electron donation decreased and the p*K*a value decreased. Based on this, the author further synthesized azobenzene **19** by forming dioxane to limit the collision between the *meta* and *para* positions, and introducing a five-membered ring at the *para* position to avoid the collision of the H on the ring with dioxane in space [37]. Thus, the maximum absorption wavelength of **19** was obtained as 697 nm, and the isomerization of **19** could be driven by 720 nm near infrared light under physiological conditions.

### 2.7. $BF_2$ azobenzenes

In 2012, Aprahamian *et al*. found that azobenzene **20** for which the azo group complexed with $BF_2$ can not only achieve *cis*-*trans* isomerization in the visible region, but also has a longer half-life of 12.5 h compared to other pseudostilbenes [38]. In dichloromethane, the $\lambda_{max}$ values of *trans*-**20** and *cis*-**20** were 530 nm and 480 nm, respectively. To further redshift the absorption wavelength by extending the conjugate system of **20**, Aprahamian *et al*. synthesized **21** that shows a slight redshift in its maximum absorption wavelength from that of **20** [39]. The half-life of the switch **21** could be adjusted by adjusting the concentration of self-aggregation, allowing half-life varying from a few seconds to a few days. Moreover, in 2014, the author continued to design a series of $BF_2$ azobenzene to introduce an electron-donating group on the *para*-position or *ortho*-position, and pointed out that the *para*-position substituent exerts a stronger effect than the *ortho*-position substituent [40]. After *para*-substitution, the absorption band of the $BF_2$ azobenzene was transferred to the red or even near-infrared region, so that the isomerization could be directly and effectively activated using near-infrared light. The maximum absorption wavelength of six-membered ring or acyclic substituted $BF_2$ azobenzene **22** is in the region of 652−681 nm. When the *para* position is substituted with pyrrole, the maximum absorption wavelength of the formed azobenzene **23** is further red-shifted to 690 nm, and the photoswitch **23** can be activated with 730 nm near-infrared light.

### 2.8. Heterocyclic azobenzenes

In addition to substitution by different substituents on azobenzene, the benzene ring can also be replaced with other heterocycles. While the use of heteroatoms often leads to unexpected properties [41], the photoisomerization of heterocyclic azobenzenes has only recently begun to attract attention with studies of heterocycles such as pyridine [42,43], imidazole [44–46], pyrrole [3,47], indole [48], indazole [49], pyrimidine [50,51],

pyrazole [3,52,53], and thiazole [54]. Compared to azobenzenes, heterocyclic azo compounds can also adjust the energy barrier through hydrogen bonds or coordination bonds [48,55,56], and their half-life values range from picoseconds to thousands of days.

To date, most heterocyclic azobenzenes have shown the $\lambda_{max}$ in the 310−362 nm range with illumination at 340 nm used to drive the *trans*-to-*cis* isomerization [3,44,46,55,57]. The type and number of heterocycles, as well as the substituents on the heterocyclic azobenzene will affect the photophysical properties of the heterocyclic azobenzenes.

When one of the benzene rings is replaced by a heterocyclic ring, due to the influence of the characteristics of the heterocyclic ring, the formed heterocyclic azobenzene may be driven by visible light. For example, when a benzene ring is replaced by pyrrole or indole, molecules **24** [3] and **25** [48] are formed, respectively. Since for both of these, the $\lambda_{max}$ is approximately 380 nm, **24** and **25** can also be excited by illumination at approximately 400 nm. When a benzene ring is replaced by 6-azopurine (**26**), $\lambda_{max}$ is in the range of 520−580 nm and photoisomerization of *trans*-**26** occurs under the irradiation of 530 nm light [58].

In addition, replacement of two benzene rings with heterocycle of the same type (**27**, **28**, **29**) [59] or with different types of heterocycles (**30**, **31**, **32**) [54] can also lead to a redshift of the maximum absorption wavelength to the visible light region. Addition of appropriate substituents can also modify the corresponding heterocyclic azobenzenes to enable excitation by visible light. In the structure of **33**, the naphthalene ring replaces the benzene ring in the original azoimidazole [45]. As the conjugated system increases, the absorption is redshifted to 390 nm. In molecules **34** and **35**, strong electron-donating amino groups are introduced into the structure, also causing the absorption wavelengths of these molecules to redshift [53,60]. Taking into account the electron-withdrawing or electron-donating properties of the heterocyclic ring itself, additional push-pull azo derivatives can also be constructed to achieve the same effect. Pyrrole can be regarded as an electron-donating group, and an electron-withdrawing nitro group is introduced on the other side of the benzene ring to obtain **36**, leading to the redshift of the $\lambda_{max}$ of **36** to the green light region [54]. While pyridine salt can be regarded as an electron-withdrawing group, an amino group is introduced on another benzene ring (**37**), and the $\lambda_{max}$ of **37** is redshifted to 560 nm [43].

## 3. The addition of upconversion nanoparticles

Upconversion is the continuous emission of light with a wavelength shorter than the excitation wavelength under the excitation of long-wavelength light and is an anti-Stokes type emission [61]. The upconversion nanoparticles can absorb near-infrared light and transfer the excited state energy to the azo core through energy transfer to promote the isomerization of the azobenzene. The introduction of upconversion nanoparticles endows the corresponding azo derivatives with the potential for indirect excitation by near-infrared light, thereby providing greater convenience for treatment and imaging [62].

Ju *et al*. reported on an azobenzene modified with upconversion nanoparticles (UCNPs), UCNPs-$LA_{Azo}BC_{Azo}$/DOX-TAT-HA ($UL_{Azo}TH$/DOX). Under 980 nm near infrared light illumination, UCNPs emitted UV light and blue light to promote the continuous photoisomerization of azobenzene, and azobenzene acted as an impeller pump to trigger circulating DNA hybridization or dehybridization to control doxorubicin (DOX) release (Fig. 4a). In a relatively short period of time, the system showed 86.7% DOX release that in turn gave rise to a good inhibitory effect on tumors (Fig. 4b) [63].

Cheng *et al*. proposed UCNPs@PAA-Azo [64]. In this case, UCNPs emitted 365 nm UV light and 475 nm blue light as well as 1345 nm NIR-II light under the excitation by 808 nm laser (Fig. 4c). The PAA-Azo simultaneously absorbed blue and UV light, and exhibited reversible *trans-cis* photoisomerization. In principle, UV light and blue light can be converted into inherent vibration and heat that helped to enhance the photoacoustic signal (PA). The PA signal of UCNPs@PAA-Azo was six times higher than that of the corresponding unmodified UCNPs. Compared to the use of UCNPs only, this approach enabled high-resolution imaging of the hind limb vasculature by dual NIR-II imaging (Fig. 4d) and PA imaging (Figs. 4e–g).

## 4. The employment of two-photon absorption

In traditional optics theory, excitation is achieved by absorbing resonant single photon energy. Two-photon absorption means that the energy of the photon absorbed to the excited state is half of the energy of the corresponding single-photon transition that can achieve three-dimensional control of the same process [12,65]. And using two-photon technology, visible light or even near infrared light can be used to promote the photoisomerization of azo derivatives. Therefore, optimization of azobenzenes that can effectively respond to two-photon excitation has received extensive research attention. Specifically, the optimization of two-photon absorption usually is based on either one of two methods:

(1) Push-pull azobenzenes. The combination of azobenzene derivatives and two-photon technology has long been reported in biological research. The near-infrared two-photon excitation process can be used to replace the short wavelength single-photon absorption to realize *trans*-to-*cis* isomerization of this type of azobenzenes. For example, azobenzene derivatives can be introduced into photoconversion tethered ligands (PTLs) to construct light-gated glutamate receptors (LiGluR) that can regulate neurons under the action of near-infrared two-photon excitation. The most classic structure constructed by this method is the maleimide-azobenzene-glutamate photoswitch (MAG, **38**). Under the stimulation of 380 nm single-photon absorption or 800 nm two-photon absorption, *trans*-**38** is transformed into *cis*-**38**. The *cis*-**38** of the system brings the ligand close to the binding site and induces glutamate recognition, leading to the opening of the ion channel and ultimately produces a light-induced neuronal excitatory potential. Subsequently, the metastable *cis*-isomer allows the process of reversal and the restoration of the original closed channel (Fig. 5a). Then, the researchers replaced the amide group on **38** with an amino group to obtain **39** that also displays a sufficiently strong push-pull behavior to enhance its two-photon absorption cross-section. **39** can be driven by 425 nm single-photon absorption or 900 nm two-photon absorption. Based on these results, an additional two-photon absorption antenna was introduced in **40** in an attempt to further enhance its two-photon absorption. Although the two-photon cross-section of **38** is smaller than those of **39** and **40**, due to its thermal stability, **38** ($\tau_{1/2}$ = 25.5 min) displays a higher long-term two-photon response than **39** ($\tau_{1/2}$ = 118 ms) and **40** ($\tau_{1/2}$ = 96 ms) (Fig. 5b) [66].

Therefore, ensuring the thermal stability of azobenzene derivatives is a prerequisite for further improving their two-photon response characteristics. In compound **41**, a weak electron donating group and a weak electron withdrawing group are introduced at the *para* positions of the azobenzene structure. To further increase the charge asymmetry and maintain the thermal stability, a fluorine atom is introduced at the *ortho* position, thereby forming molecule **42** that is a push-pull azobenzene with slow thermal isomerization. The 780 nm near-infrared two-photon response and the 405 nm single-photon response of **42** are almost the same in cells and tissues (Fig. 5c), and **42** can return to the *trans*

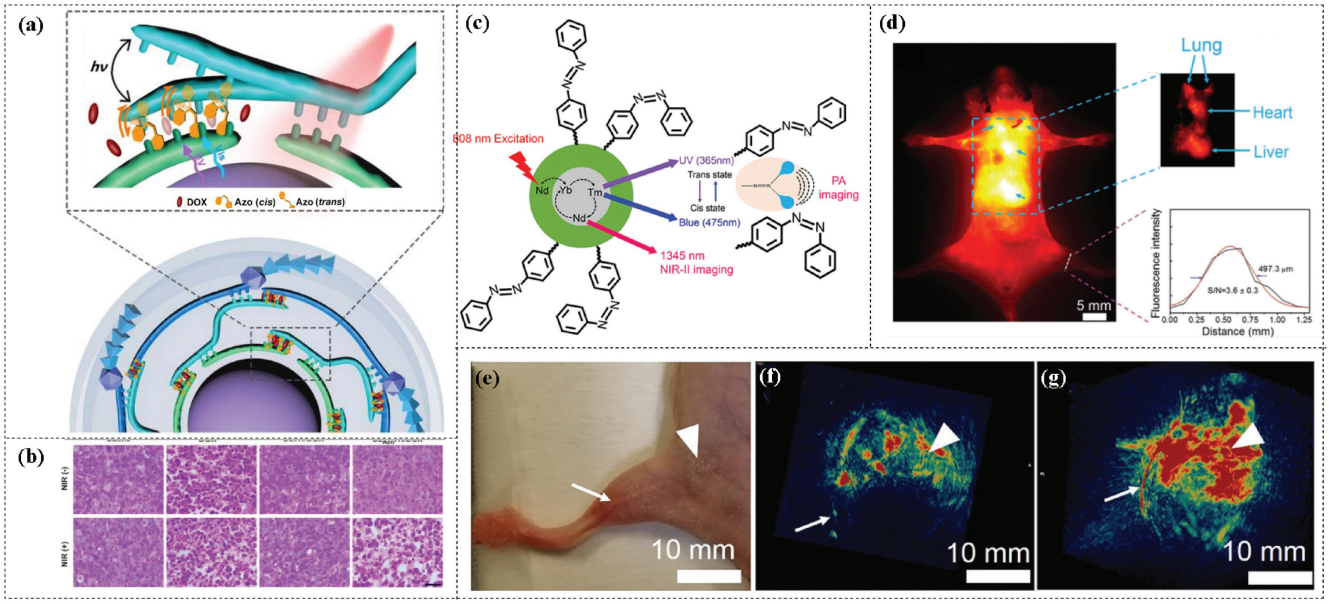


**Fig. 4.** (a) Schematic diagram of UCNPs-LAAzoBCAzo/DOX-TAT-HA (ULAzoTH/DOX). The ULAzoTH/DOX is fabricated with azobenzene-functionalized DNA strands for efficient and controllable drug release through the photoisomerization of azobenzene fueled by simultaneous UV and blue emissions of UCNPs under 980 nm irradiation. (b) Histological observations of tumor tissues after treatment with saline, DOX, UCNPs-LABC/DOX-TAT-HA(ULTH/DOX) and ULAzoTH/DOX and then near-infrared light irradiation. (a and b) Copied with permission [63]. Copyright 2019, John Wiley and Sons. (c) The main mechanism of UCNPs@PAA-Azo, the UCNPs simultaneously emit UV and blue light as well as NIR-II light under excitation from an 808 nm laser. The absorption of UV and blue light leading to the *cis-trans* isomerization contributes to an enhancement in PA intensity, and the NIR-II emission at 1345 nm can be used for biological imaging with high sensitivity. (d) NIR-II image of C57BL/6 mouse *in vivo*. (e) Digital photograph of C57BL/6 mouse showing region photographed in NIR-II windows. (f) 3D volume rendering of PA of the vasculature of the hind limb of a mouse after injection UCNPs in 30 min. (g) 3D volume rendering of PA of the vasculature of the hind limb of a mouse after injection UCNPs@PAA-Azo in 30 min. (c-g) Copied with permission [64]. Copyright 2019, John Wiley and Sons.

structure after illumination at 514 nm or in the dark. At the same time, in the *C. elegans in vivo* experiment, a single pair of the PLML/R tactile receptor neurons near the tail of *C. elegans* can be differentially activated by this method (Fig. 5d), paving the way for the future imaging of a complete three-dimensional neural circuit [67].

(2) Introduction of two-photon absorption chromophore. To obtain a suitable two-photon absorption antenna, generally the emission of the chromophore must overlap with the absorption of the azobenzene core, and the two-photon absorption cross-section must be high.

Triarylamine is a traditional two-photon antenna, Hecht *et al.* extended its maximum absorption wavelength to 380 nm by extending its conjugate system. The modified triarylamine was then connected to the *meta* position of tetra-*o*-fluoroazobenzene to ensure the decoupling of the ground state. These two components of **43** showed different selective excitation and spectral properties (Fig. 5e) [68], and the triarylamine emission and the *cis*-**43** nuclear absorption spectrum overlapped, favoring the realization of energy transfer and allowing the use of low-energy near-infrared two-photon (750 nm) absorption to achieve *cis*-to-*trans* isomerization. Then, *trans*-**43** could be quantitatively isomerized using single-photon visible light (510 nm). The thermal half-life of **43** at room temperature exceeded 500 days.

## 5. Indirect excitation in combination with metal sensitizer

In addition, if a metal sensitizer is introduced into azobenzene, the molecule will have some unique properties. On the one hand, coordination can improve the thermal stability of the metastable state. On the other hand, in addition to the direct stimulation of the azo group, *cis-trans* isomerization can also be performed by external stimulation (photo/electron) of metal ligands.

Here we mainly introduce two examples of azo derivatives containing metal sensitizers, namely record player azobenzene and ferrocene azobenzene.

Herges *et al.* reported Ni-porphyrin azopyridine (**44**), a record player azobenzene, that showed *trans*-to-*cis* and *cis*-to-*trans* isomerization with illumination at 500 nm and 435 nm, respectively [69,70]. The isomerization mechanism of **44** was different from that of other azobenzenes. The authors attributed this redshift of the excitation wavelength to an energy transfer from the $\pi \rightarrow \pi^*$ excited state of the porphyrin (Q band) to the $\pi \rightarrow \pi^*$ state of the azopyridine. *cis*-**44** was stabilized by pyridine coordination with nickel porphyrin and was stable for several weeks (Fig. 6a).

Ferrocene is introduced into azobenzene to obtain structure **45,** and the corresponding isomerization process involves the modification of the oxidation state of ferrocene [71]. The metal-to-ligand charge transfer transition of **45** occurred at the wavelength of approximately 450 nm, and **45** was irradiated with 546 nm green light to achieve *trans*-to-*cis* photoisomerization. Subsequently, the $Fe^{2+}$ in the ferrocene group was oxidized to $Fe^{3+}$, and *cis*-to-*trans* isomerization occurred under illumination with the same green light (Fig. 6b).

## 6. Conclusion

Azo derivatives are photoswitches with wide tunability of structure and properties that have been long investigated in order to optimize their external stimulation conditions (excitation wavelength, light intensity, lighting time) and internal response performance (addressability, thermal stability, efficiency, reliability) to meet the needs of different fields. Current research has tended to focus on the use of different types of dyes for the near infrared region of the electromagnetic spectrum [72–78], so that they can be excited by visible light or even near infrared light to meet the needs of

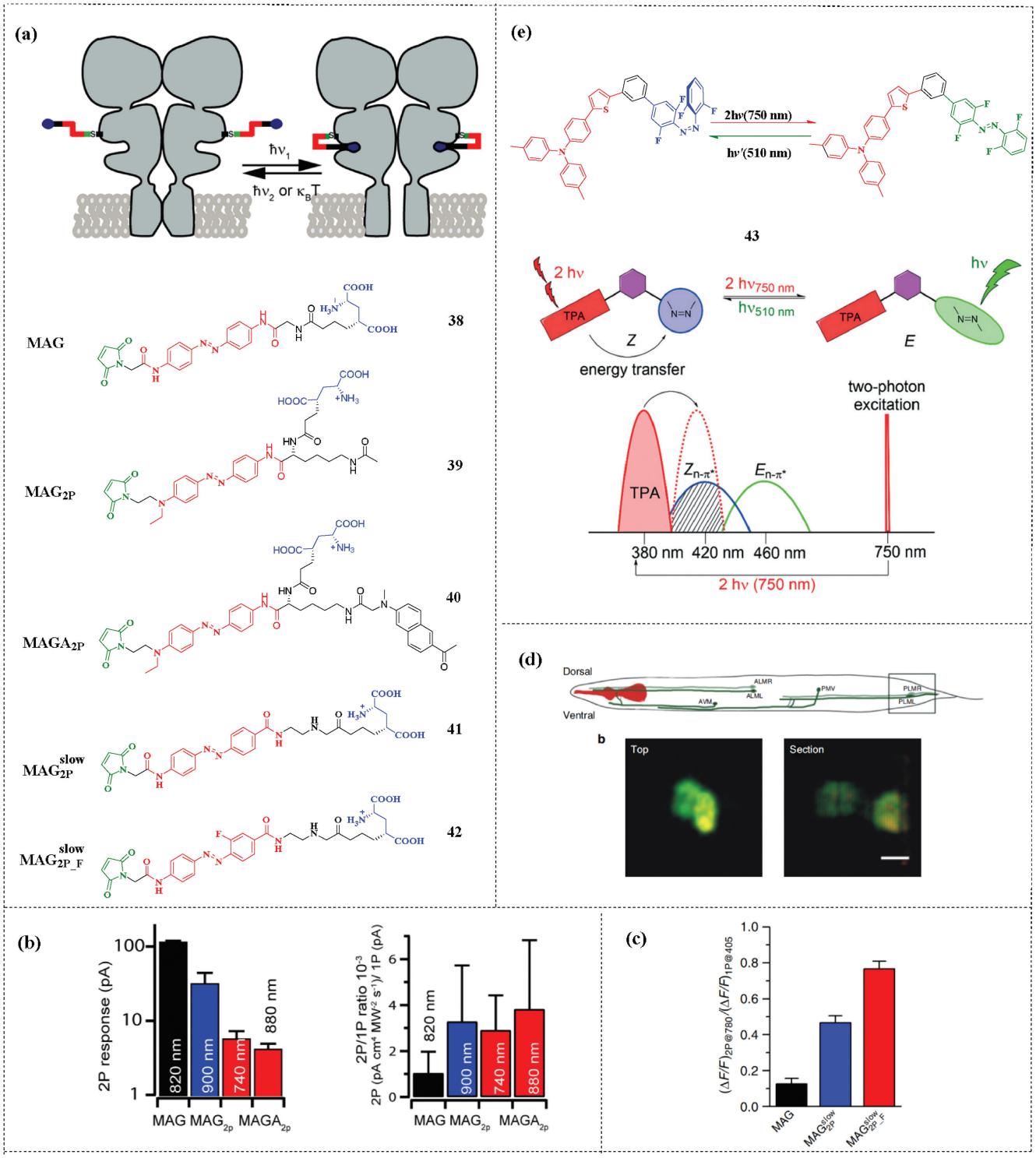


**Fig. 5.** (a) The operation mechanism of photoswitchable tethered ligands (PTLs) on light-gated glutamate receptors (LiGluR), which consists of three parts: a glutamic acid ligand, an azobenzene core, and a maleimide group that binds to a cysteine residue genetically engineered in the receptor. Single-photon or near-infrared two-photon induces glutamate recognition and opens the channel in the *cis*-isomer, resulting in ion flow through the membrane. It is then restored to *trans*-isomer by visible light excitation or thermal deisomerization. (b) The absolute two-photon (2P) response at the best wavelengths and the ratio of two-photon to single-photon response (2P/1P) for MAG (**38**), MAG2p (**39**) and MAGA2p (**40**). For MAGA2p (**40**) values are given for sensitized (λ = 740 nm) and direct (λ = 880 nm) azobenzene excitation. (a and b) Copied with permission [66]. Copyright 2014, American Chemical Society. (c) Ratio between the two- and one-photon responses (2P/1P) for MAG (**38**), MAG$^{\text{Slow}}_{\text{2P}}$ (**41**) and MAG$^{\text{Slow}}_{\text{2P_F}}$ (**42**). (d) Schematic representation of touch receptor neurons (TRNs) in *C. elegans*. Microphotograph of an animal expressing LiGluR-mCherry (red) and GCaMP6s (green). Top and lateral section view of TRN from the tail. (c and d) Copied with permission [67]. Copyright 2019, Springer Nature. (e) Triarylamine-azobenzene **43**. Illustration of the working principle of *cis*-to-*trans* isomerization based on 750 nm two near-infrared photon sensitization and direct drive of *trans*-to-*cis* photoisomerization with 510 nm. Copied with permission [68]. Copyright 2019, John Wiley and Sons.

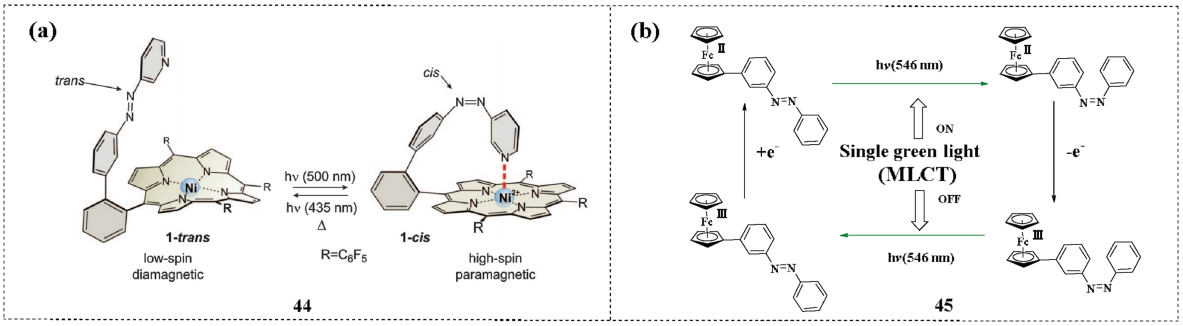


**Fig. 6.** (a) Reversible light-induced switching of azopyridine functionalized Ni-porphyrin **44**. Copied with permission [69]. Copyright 2011, The American Association for the Advancement of Science. (b) Ferrocene azobenzene **45** undergoes *trans*-to-*cis* isomerization under the green light, and the same green light induces *cis*-to-*trans* isomerization in oxidized ferrocene azobenzene. Copied with permission [71]. Copyright 2002, American Chemical Society.

biological imaging. Therefore, here we summarized the structural characteristics of the azo derivatives driven by visible light that have been explored in recent years. We found that there are four approaches for achieving visible light azo photoswitches: (1) modification of different substituents to enable direct excitation by visible light or near-infrared light to produce compounds such as *o*-halogen azobenzene, bridged azobenzenes, *o*-methoxy azobenzene, push-pull azobenzenes, protonated azobenzene, heterocyclic azobenzenes, and $BF_2$ azobenzene, (2) the addition of upconversion nanoparticles, (3) the employment of two-photon absorption, (4) indirect excitation in combination with metal sensitizer.

Each method has its own advantages and disadvantages. Generally, when azobenzene is directly modified using different substituents, both the thermal stability and excitation wavelength of the metastable state of the obtained azo derivative can be enhanced, while when a combination with nonlinear optical method, although longer excitation wavelengths can be obtained for example through the near-infrared two-photon absorption, the thermal relaxation rate is relatively high and most of the properties of the photoswitch are not as good as those obtained for single-photon excitation. Therefore, different types of azo derivatives can be selected according to the needs of different fields. Several problems still remain and must be solved urgently to enable the further use of azobenzene photoswitches. For example, the structure of heterocyclic azobenzene often has special properties, the existing research on the structure of heterocyclic azobenzene is not sufficiently thorough, and further research is needed to explore its characteristics. Additionally, further design of azo photoswitches using near-infrared light is necessary to achieve two-way steady-state modification. These issues require in-depth exploration in future research.

## Declaration of competing interest

The authors report no declarations of interest.

## Acknowledgments

This work was financially supported by the National Natural Science Foundation of China (Nos. 21676113, 21772054), Distinguished Young Scholar of Hubei Province (No. 2018CFA079), the 111 Project (No. B17019), Scholar Support Program of CCNU (No. 0900-31101090002), the Research Fund Program of Guangdong Key Laboratory of Radioactive and Rare Resource Utilization (No. 2018B030322009). The study was supported by Ministry of Education Key Laboratory for the Synthesis and Application of Organic Functional Molecules (No. KLSAOFM2012), Hubei University, China, Excellent Doctorial Dissertation Cultivation Grant of CCNU from the Colleges' Basic Research and Operation of MOE (No. 2019YBZZ029).

## References

[1] G.S. Hartley, Nature 140 (1937) 281.
[2] D.J. van Dijken, P. Kovaříček, S.P. Ihrig, et al., J. Am. Chem. Soc. 137 (2015) 14982–14991.
[3] C.E. Weston, R.D. Richardson, P.R. Haycock, et al., J. Am. Chem. Soc. 136 (2014) 11878–11881.
[4] K. Hüll, J. Morstein, D. Trauner, Chem. Rev. 118 (2018) 10710–10747.
[5] J.B. Trads, K. Hüll, B.S. Matsuura, L. Laprell, et al., Angew. Chem. Int. Ed. 58 (2019) 15421–15428.
[6] S. Li, G. Han, W. Zhang, Macromolecules 51 (2018) 4290–4297.
[7] J. Luo, S. Samanta, M. Convertino, N.V. Dokholyan, et al., ChemBioChem 19 (2018) 2178–2185.
[8] A. Myrhammar, D. Rosik, A.E. Karlström, Bioconjugate Chem. 31 (2020) 622–630.
[9] Y.S. Chen, L. Li, W.J. Chen, et al., Chin. Chem. Lett. 30 (2019) 1353–1360.
[10] W.J. Chen, Y.L. Pan, J.H. Chen, et al., Chin. Chem. Lett. 29 (2018) 1429–1435.
[11] Y.P. Wang, Z.X. Zhang, M. Xie, et al., Dyes Pigments 129 (2016) 100–108.
[12] D. Bléger, S. Hecht, Angew. Chem. Int. Ed. 54 (2015) 11338–11349.
[13] H.M.D. Bandara, S.C. Burdette, Chem. Soc. Rev. 41 (2012) 1809.
[14] D.J. Warner, K.S. Keane, S.C. Blackstock, Bridged azobenzenes and their chemical applications, in: Z. Rappoport (Ed.), PATAI'S Chemistry of Functional Groups, John Wiley & Sons Inc., Hoboken, New Jersey, 2019, pp. 1–35.
[15] D. Bléger, J. Schwarz, A.M. Brouwer, et al., J. Am. Chem. Soc. 134 (2012) 20597–20600.
[16] C. Knie, M. Utecht, F. Zhao, et al., Chem. Eur. J. 20 (2014) 16492–16501.
[17] S. Samanta, A.A. Beharry, O. Sadovski, et al., J. Am. Chem. Soc. 135 (2013) 9777–9784.
[18] D.B. Konrad, G. Savasci, L. Allmendinger, et al., J. Am. Chem. Soc. 142 (2020) 6538–6547.
[19] C.L. Forber, E.C. Kelusky, N.J. Bunce, et al., J. Am. Chem. Soc. 107 (1985) 5884–5890.
[20] R. Siewertsen, H. Neumann, B. Buchheim-Stehn, et al., J. Am. Chem. Soc. 131 (2009) 15594–15595.
[21] M. Hammerich, C. Schütt, C. Stähler, et al., J. Am. Chem. Soc. 138 (2016) 13111–13114.
[22] M.S. Maier, K. Hüll, M. Reynders, et al., J. Am. Chem. Soc. 141 (2019) 17295–17304.
[23] S. Li, N. Eleya, A. Staubitz, Org. Lett. 22 (2020) 1624–1627.
[24] H. Sell, C. Näther, R. Herges, Beilstein J. Org. Chem. 9 (2013) 1–7.
[25] R. Herges, W. Moormann, T. Tellkamp, et al., Angew. Chem. Int. Ed. 59 (2020) 1–7.
[26] P. Lentes, E. Stadler, F. Röhricht, et al., J. Am. Chem. Soc. 141 (2019) 13592–13600.
[27] A.A. Beharry, O. Sadovski, G.A. Woolley, J. Am. Chem. Soc. 133 (2011) 19684–19687.
[28] S. Samanta, T.M. McCormick, S.K. Schmidt, et al., Chem. Commun. 49 (2013) 10314–10316.
[29] O. Sadovski, A.A. Beharry, F. Zhang, et al., Angew. Chem. Int. Ed. 48 (2009) 1484–1486.
[30] Z. Ahmed, A. Siiskonen, M. Virkki, et al., Chem. Commun. 53 (2017) 12520–12523.
[31] M. Dong, A. Babalhavaeji, S. Samanta, et al., Acc. Chem. Res. 48 (2015) 2662–2670.
[32] J.S. Zhu, J.M. Larach, R.J. Tombari, et al., Org. Lett. 21 (2019) 8765–8770.
[33] M.A. Kienzler, A. Reiner, E. Trautman, et al., J. Am. Chem. Soc. 135 (2013) 17683–17686.
[34] S. Samanta, A. Babalhavaeji, M.X. Dong, et al., Angew. Chem. Int. Ed. 52 (2013) 14127–14130.
[35] C.E. Weston, R.D. Richardson, M.J. Fuchter, Chem. Commun. 52 (2016) 4521–4524.

[36] M. Dong, A. Babalhavaeji, M.J. Hansen, et al., Chem. Commun. 51 (2015) 12981–12984.
[37] M. Dong, A. Babalhavaeji, C.V. Collins, et al., J. Am. Chem. Soc. 139 (2017) 13483–13486.
[38] Y. Yang, R.P. Hughes, I. Aprahamian, J. Am. Chem. Soc. 134 (2012) 15221–15224.
[39] H. Qian, Y.Y. Wang, D.S. Guo, et al., J. Am. Chem. Soc. 139 (2017) 1037–1040.
[40] Y. Yang, R.P. Hughes, I. Aprahamian, J. Am. Chem. Soc. 136 (2014) 13190–13193.
[41] F. Deng, Z.C. Xu, Chin. Chem. Lett. 30 (2019) 1667–1681.
[42] J. Garcia-Amorós, S. Nonell, D. Velasco, Chem. Commun. 47 (2011) 4022–4024.
[43] J. Garcia-Amorós, S. Nonell, D. Velasco, Chem. Commun. 48 (2012) 3421–3423.
[44] J. Otsuki, K. Suwa, K. Narutaki, et al., J. Phys. Chem. A 109 (2005) 8064–8069.
[45] J. Otsuki, K. Suwa, K.K. Sarker, et al., J. Phys. Chem. A 111 (2007) 1403–1409.
[46] T. Wendler, C. Schütt, C. Näther, et al., J. Org. Chem. 77 (2012) 3284–3287.
[47] J.A. Balam-Villarreal, B.J. López-Mayorga, D. Gallardo-Rosas, et al., Org. Biomol. Chem. 18 (2020) 1657–1670.
[48] N.A. Simeth, S. Crespi, M. Fagnoni, et al., J. Am. Chem. Soc. 140 (2018) 2940–2946.
[49] A. Rennhack, E. Grahn, U.B. Kaupp, et al., ACS Chem. Biol. 12 (2017) 2952–2957.
[50] E. Procházková, L. Čechová, J. Kind, et al., Chem. Eur. J. 24 (2018) 492–498.
[51] J. Garcia-Amorós, M. Díaz-Lobo, S. Nonell, et al., Angew. Chem. Int. Ed. 51 (2012) 12820–12823.
[52] S. Devi, M. Saraswat, S. Grewal, et al., J. Org. Chem. 83 (2018) 4307–4322.
[53] K. Rustler, P. Nitschke, S. Zahnbrecher, et al., J. Org. Chem. 85 (2020) 4079–4088.
[54] J. Garcia-Amorós, M.C.R. Castro, P. Coelho, et al., Chem. Commun. 49 (2013) 11427–11429.
[55] J. Calbo, C.E. Weston, A.J.P. White, et al., J. Am. Chem. Soc. 139 (2017) 1261–1274.
[56] S. Crespi, N.A. Simeth, B. König, Nat. Rev. Chem. 3 (2019) 133–146.
[57] P. Kumar, A. Srivastava, C. Sah, et al., Chem. Eur. J. 25 (2019) 11924–11932.
[58] D. Kolarski, W. Szymanski, B.L. Feringa, Org. Lett. 19 (2017) 5090–5093.
[59] A.D.W. Kennedy, I. Sandler, J. Andréasson, et al., Chem. Eur. J. 26 (2020) 1103–1110.
[60] E. Procházková, L. Čechová, J. Kind, et al., Chem. Eur. J. 24 (2018) 492–498.
[61] D.S. Wang, W.F. Zhao, Q. Wei, C.C. Zhao, et al., ChemPhotoChem 2 (2018) 403–415.
[62] C.X. Yan, L.M. Shi, Z.Q. Guo, et al., Chin. Chem. Lett. 30 (2019) 1849–1855.
[63] Y. Zhang, Y. Zhang, G.B. Song, et al., Angew. Chem. Int. Ed. 58 (2019) 18207–18211.
[64] S.Q. He, J. Song, J.F. Liu, et al., Adv. Opt. Mater. 7 (2019) 1900045.
[65] D. Chen, W.J. Qin, H.X. Fang, et al., Chin. Chem. Lett. 30 (2019) 1738–1744.
[66] M. Izquierdo-Serra, M. Gascón-Moya, J.J. Hirtz, et al., J. Am. Chem. Soc. 136 (2014) 8693–8701.
[67] G. Cabré, A. Garrido-Charles, M. Moreno, et al., Nat. Commun. 10 (2019) 907.
[68] J. Moreno, M. Gerecke, L. Grubert, et al., Angew. Chem. Int. Ed. 55 (2016) 1544–1547.
[69] S. Venkataramani, U. Jana, M. Dommaschk, et al., Science 331 (2011) 445–448.
[70] M. Dommaschk, M. Peters, F. Gutzeit, et al., J. Am. Chem. Soc. 137 (2015) 7552–7555.
[71] M. Kurihara, A. Hirooka, S. Kume, et al., J. Am. Chem. Soc. 124 (2002) 8800–8801.
[72] D.Y. Li, W.J. Chen, S.H. Liu, et al., Chin. Chem. Lett. 30 (2020) 2891–2896.
[73] W.J. Chen, C. Zhang, X. Han, et al., J. Org. Chem. 84 (2019) 14498–14507.
[74] F.Y. Ye, W.J. Chen, Y.L. Pan, et al., Dyes Pigments 171 (2019) 107746.
[75] J. Xu, L. Shang, Chin. Chem. Lett. 29 (2018) 1436–1444.
[76] M.P. O'Hagan, J. Ramos-Soriano, S. Haldar, et al., Chem. Commun. 56 (2020) 5186–5189.
[77] H. Zhou, Y.L. Xiao, X.C. Hong, Chin. Chem. Lett. 29 (2018) 1425–1428.
[78] L.J. Tang, J.Y. Xia, K.L. Zhong, et al., Dyes Pigments 178 (2020) 108379.